



Evaluation of vehicular pollution levels using line source model for hot spots in Muscat, Oman

Patrick Amoatey¹ · Hamid Omidvarborna^{1,2} · Mahad Said Baawain¹ · Abdullah Al-Mamun¹

Received: 24 February 2020 / Accepted: 7 May 2020 / Published online: 1 June 2020
© Springer-Verlag GmbH Germany, part of Springer Nature 2020

Abstract

A detailed investigation was carried out to assess the concentration of near-road traffic-related air pollution (TRAP) using a dispersion model in Muscat. Two ambient air quality monitoring (AQM) stations were utilized separately at six locations near major roadways (each location for 2 months) to monitor carbon monoxide (CO) and nitrogen oxides (NO_x). The study aimed to measure the concentration of near-road TRAP in a city hot spots and develop a validated dispersion model via performance measures. The US Environmental Protection Agency (US EPA) Line Source Model was implemented in which the pollutant emission factors were obtained through Comprehensive Modal Emission Model (CMEM) and Computer Programme to calculate Emissions from Road Transport (COPERT) model. Traffic data of all vehicle categories under normal driving conditions including average vehicle speed limits and local meteorological conditions were included in the modeling study. The analysis of monitoring data showed that hourly (00:00 to 23:00) concentrations of CO were within the US EPA limits, while NO_x concentration was exceeded in most locations. Also, the measured pollutant levels were consistent with hourly peak and off-peak traffic volumes. The overall primary statistical performance measures showed that COPERT model was better than CMEM due to the high sensitivity of CMEM to the local meteorological factors. The best fractional bias (0.47 and 0.39), normalized mean square error (0.44 and 0.50), correlation coefficient (0.64 and 0.70), geometric mean bias (1.07 and 1.57), and geometric variance (2.00 and 2.32) were obtained for CO and NO_x, respectively. However, the bootstrap 95% CI estimates over normalized mean square error, fractional bias, and correlation coefficient for COPERT and CMEM were found to be statistically significant from 0 in the case of combined model comparison across all the traffic locations for both CO and NO_x. In overall, certain roads showed weak performance mainly due to the terrain features and the lack of reliable background concentrations, which need to be considered in the future study.

Keywords Emissions · Road traffic · Air pollution · CMEM · COPERT IV · AERMOD

Introduction

Near-road traffic-related air pollution (TRAP) is one of the most serious public health concerns facing many countries

due to emissions of several toxic ambient air pollutants from on-road vehicles (Liang et al. 2018; Mannucci and Franchini 2017; Munir and Habeebullah 2018). Studies have shown that exposure to TRAP has resulted in the incidence of pulmonary diseases such as abnormal lung function (Bowatte et al. 2018), incident of cardiovascular diseases (Cai et al. 2018), respiratory cancer (Ribeiro et al. 2019), childhood asthma (Khreis et al. 2018), and diabetes mellitus (Pedersen et al. 2017). World Health Organization (WHO) estimated about 12–70% of total ambient air pollution levels in African and Asian (especially Middle Eastern) countries due to road TRAP (WHO 2019). This is mainly due to the increase in motorization rate, lack of adequate green infrastructure, the absence of engine powered electric vehicles, and urban development in nearby roadways, whereas TRAP comes into play (Korfant and Gogola 2019; Omidvarborna et al. 2018; Rosenlieb et al.

Responsible Editor: Gerhard Lammel

✉ Mahad Said Baawain
msab@squ.edu.om

¹ Department of Civil and Architectural Engineering, College of Engineering, Sultan Qaboos University, P.O. Box 33, Al-Khoudh, 123 Muscat, Sultanate of Oman

² Global Centre for Clean Air Research, Department of Civil and Environmental Engineering, Faculty of Engineering and Physical Sciences, University of Surrey, Guildford, Surrey GU2 7XH, UK

2018; Zhou and Gao 2018). Among the gaseous pollutants, nitrogen oxides (NO_x) and carbon monoxide (CO) are the most common forms of near-road TRAP (Bodisco et al. 2019; Gokhale and Pandian 2007; Ko et al. 2019; López-Pérez et al. 2019; Triantafyllopoulos et al. 2019; Wallace et al. 2012). Thus, accurate measurements and model estimations are the fundamental factors of reducing the incidents of TRAP morbidity and mortality through policy formulations and mitigation actions (US EPA 2019).

Assessment of TRAP has well explored in parts of the world. For example, Perugu (2019) enhanced the emission rates estimates of CO, NO_x, and hydrocarbons (HC) for light-duty vehicles (LDV) in India based on local driving conditions by adapting the United States Environmental Protection Agency (US EPA's) Motor Vehicle Emission Simulator (MOVES) model. Gibson et al. (2013) found a good model performance between US EPA Regulatory Model (AERMOD) dispersion model output and that of the measured field data for near-road traffic-related particulate matter (PM) and sulfur dioxide (SO₂) concentration levels in Nova Scotia, Canada. Also, many European cities have also used similar TRAP modeling approach such as URBAN AIR (URBAIR) and Urban Air Quality Model (ADMS-Urban) models in evaluating the exposure concentrations of several air pollutants mostly NO_x, PM, HC, and black carbon (BC) due to road traffic activities (Borrego et al., 2016; Mallet et al., 2018).

The literature review showed that the concentration levels of gaseous TRAP (e.g., CO and NO_x) near major roadway were poorly investigated in Oman. In such environments with a high level of solar radiation, emission of TRAP is considered as the major challenge as it readily causes the production of ground-level O₃ (Baawain and Al-Serhi 2014). The first and only study in Muscat was conducted by Abdul-Wahab and Fadlallah (2014), in which the California Puff model (CALPUFF) model was employed in simulating concentration of NO_x and CO in a single road within Sultan Qaboos University. This study could not validate the predicted concentrations with the field data which were important in determining the prediction, performance, and the association of the modeled results with the measured data (Kadiyala and Kumar 2012). In addition, the study was limited to a local area, where the majority of vehicles were listed as LDV. Hence, the model could not predict busy roadways with different vehicular volume levels and vehicle categories (heavy-duty vehicles (HDV) and LDV). The second TRAP modeling study was focused only on the modeling of NO_x and CO in Salalah city, Oman, by comparing the predicted pollutant concentration levels between monsoon and non-monsoon seasons with CALPUFF. The estimates were made during only peak and off-peak traffic volumes and did not present average traffic flows and emission in the Salalah city. Also, the reliability of the model in determining the predicted air pollutant

concentration levels was not validated due to the lack of measured data (Charabi et al. 2018).

Most developed countries have established their own TRAP emission rate database for detailed road traffic emission modeling (Borrego et al. 2016; Milando and Batterman 2018; Righi et al. 2009; Wallace et al. 2012). However, literature review studies in Oman revealed poor background study due to lack of time-series air quality monitoring (AQM) data, local meteorological data, reliable emission rate database, and well-fitted models. This study aimed to evaluate the performance of two emission rate models (CComputer Programme to calculate Emissions from Road Transport (COPERT IV) and Comprehensive Modal Emission Model (CMEM)) to predict CO and NO_x concentration levels from the near-road environment using AERMOD dispersion model. CMEM was considered for the study as it offers a flexible traffic input data requirements, including local meteorological parameters, whereas the acquired COPERT IV data presents emission factors of different vehicle categories similar to vehicle types under the current study. Both COPERT IV and CMEM are the most comprehensive emission rate models in terms of input parameters. Therefore, they can be utilized as the most reliable emission rate models for the countries with no established emission rate database.

In addition, AERMOD dispersion modeling has not been used widely for investigating traffic emissions from multiple road networks of varied vehicle volumes and types. This study monitored the gaseous TRAP at six major roadways by using two mobile ambient AQM stations for the first time in Muscat (see Fig. 1), and the developed dataset was used to validate the emission rate models, while it attempted to predict urban air quality at major hotspots.

Background

Description of the study area

This study was carried out in Muscat Governorate (23° 36' 51.5808" N, 58° 32' 43.0224" E) which is the capital city of Oman located in the northern region of the country with a total area of 1500 km² (Fig. 1) (Kwarteng et al. 2009). According to Directorate General of Meteorology (2019), mean annual precipitations, ambient temperature, and humidity levels of the Muscat are 150–750 mm, 23.1–33.6 °C, and 29–67%, respectively. Muscat is the most populated city of the country with a current estimated resident population of 1.5 million out of the total 4.6 million national population. Currently, the annual population growth rate is about 3.3–5.9% (National Centre for Statistics and Information 2018).

The rapid increase in road traffic population has been one of the major challenges by the Government of Oman, which is attributed to limited public transportation systems, subsidized

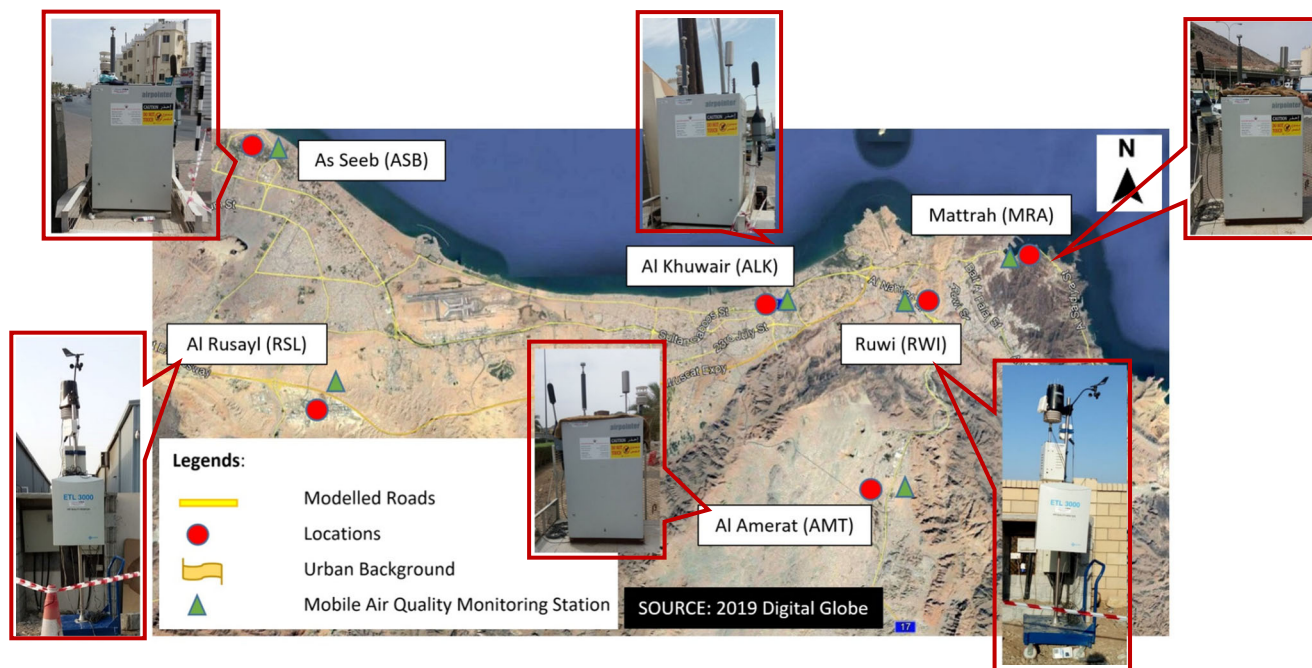


Fig. 1 A map showing road traffic air quality sampling locations in Muscat

vehicle importation taxes, and fuel prices. For example, an average of one vehicle per every household is estimated in Muscat (Amoatey and Sulaiman 2017). In addition, the number of newly registered vehicles in 2017 rose to as high as 175,266 compared to 131,700 vehicles in 2013, indicating a percentage increase of about 25% (Islam and Al-Hadrami, 2012). These have caused a high number of several LDV and HDV attributing to high air pollution levels in the major cities. The details of traffic volumes in these study are presented in “[Vehicle population and composition.](#)”

Road traffic condition in Muscat

On-road vehicle activities differ from one city to another in Oman. Currently, National Centre for Statistics and Information (NCSI) and Ministry of Transport and Communication do not have a comprehensive dataset on vehicle emission factors and vehicle kilometer traveled for different vehicle categories in Oman. But vehicle volume, distribution, and road inventories data have been a part of the 2011 national traffic survey study (Muscat Municipality 2019).

Our estimation showed that Muscat has the highest vehicle volumes compared to other cities in Oman. This is because the city served as a hub for most economic activities in the country. Majority of manufacturing companies, oil industries, government agencies, schools, hospitals, and hospitality industries are located in major industrial (Ruwi (RWI) and Rusayl (RSL)) and business (Al Khuwair (ALK), Al Amerat (AMT), A Seeb (ASB), and Muttrah (MRA)) Wilayats/town, thereby, leading to high volumes of HDV and LDV in the city, which varies in terms of vehicles types and population.

Furthermore, the strategic location of Oman sharing a border with the United Arab Emirates (UAE) and Yemen makes it efficient for HDV to transport goods and services through Muscat. Also, low vehicle occupancy rates in addition to the high temperatures in summertime (maximum of 40 °C) make personal vehicles the convenient means of transportation for individuals in Muscat (Amoatey and Sulaiman 2017). In addition, tourism is one of the emerging sources of revenue to Oman. For example, it is estimated that tourism activities contributed to the total vehicle population of 431,105 during monsoon seasons in Salalah city, a known tourist area in the southern part of the country (Muscat Municipality 2019). However, most of these visitors move back to Muscat, thereby increasing vehicle populations and emissions. All these factors have contributed to high emission levels in Muscat. Hence, to better understand the situation, this study examined on-road vehicle populations in various Wilayats in Oman and found that the highest on-road vehicle numbers and compositions are concentrated within the six main Wilayats/towns (ASB, ALK, MRA, AMT, RWI, and RSL) of Muscat.

Data and methods

Here, the study was conducted in three stages. For the first and second steps, road traffic data and location-specific meteorological data were employed to estimate traffic emission rates in each zone. Next, the ambient air pollution dispersion model was utilized to estimate the near-road pollutants concentration levels. Finally, the modeled concentrations were validated with field data through statistical analysis.

Vehicle population and composition

Annual vehicle population from Muscat Municipality was obtained based on the national traffic survey study conducted across the major Wilayats in Muscat (Muscat Municipality 2019). In order to understand the trends of vehicle volumes in Muscat, the total number of daily traffic flows from Monday to Sunday is presented in Fig. 2. There was a sharp decrease in vehicle volumes on Thursdays and Fridays as these days are the last day of the working days and first days of weekends compared to the main business days. Interestingly, though Saturdays are the weekend, yet there were high traffic flows as people visit places within the city thereby increasing the vehicle populations. As shown in Fig. 3, vehicle flows increased from 7:00 to 11:00 AM and showed a slight reduction from 17:00 to 21:00 PM during weekdays. Analysis of inter-city road traffic volumes showed that high traffic was found in ALK (16.5%), AMT (16.5%), and RSL (38.5%) compared to other Wilayats such as MRA (15%), RWI (7.1%), and ASB (6.4%) during morning time. On the other hand, in the evening time, ALK and RSL showed a higher number of vehicles as these are commercial and industrial centers with a high number of the population compared to other places (Fig. 3).

Road transport vehicles in the six major Wilayats were categorized into eight types: car, taxi, van/light goods, 2-axle truck, 3-axle truck, private and public transports, and others (i.e., those that could not fit into aforementioned classifications) as shown in Fig. 4. Despite the variations in vehicle types, the figure clearly shows that the population of cars was distributed across most of the locations. These were found mostly in business and residential areas (ALK, AMT, ASB, and MRA) where most of the vehicles are composed of cars, taxis, van/light goods, and private/public transports. Also, it could be observed that most industrial areas such as RWI (35–65%) and RSL (18–25%) had a higher proportion of 2- and 3-axle truck vehicles, respectively, than all the remaining locations where these HDV populations were found low (8–18%). Thus, data on types and numbers of vehicles within the study

locations are important in order to assess their emission levels in different Wilayats according to the number of HDV and LDV (Wen et al. 2017; Zhang et al. 2019). Since the study aimed to model emission factors of CO and NOx from these locations, the various vehicle categories were broadly classified into HDV and LDV, where the proportion of these vehicle types was used as an input parameter for the CMEM as indicated in Table 1. In addition, location-specific meteorological variables such as temperature, humidity levels, wind speed, and ambient pressure, which were obtained through ambient AQM campaigns, were incorporated into the emission rate models. The detailed description of acquiring the field data is discussed in “Emission modeling.”

Meteorological data

In this study, the surface and upper air meteorological data for January–December 2018 were obtained from Seeb International Airport (23° 35' 43" N, 58° 17' 54" E) at an elevation of 8 m. These data have been analyzed through the Meteorological Assimilation Data Ingest System (MADIS), and then they were processed further by Breeze (2019) according to US EPA (2018a) meteorological processor (AEMET) guidelines. Here, the two meteorological datasets (upper and air-surface data) processed by AERMET were used as ready input data for the models. The detailed description of the meteorological factors including land use features of Muscat acquired from Seeb International Airport is indicated in Table 2.

Air pollution data

Field data

To collect traffic air pollution data and validate the model results, a series of field measurement campaigns were conducted from January to December 2018 across the six study locations. At each location, continuous AQM data for CO and NOx were collected with AirPointer AQM station (MLU/

Fig. 2 The average daily traffic volumes, the total number of cars, in Muscat (March–May 2011)

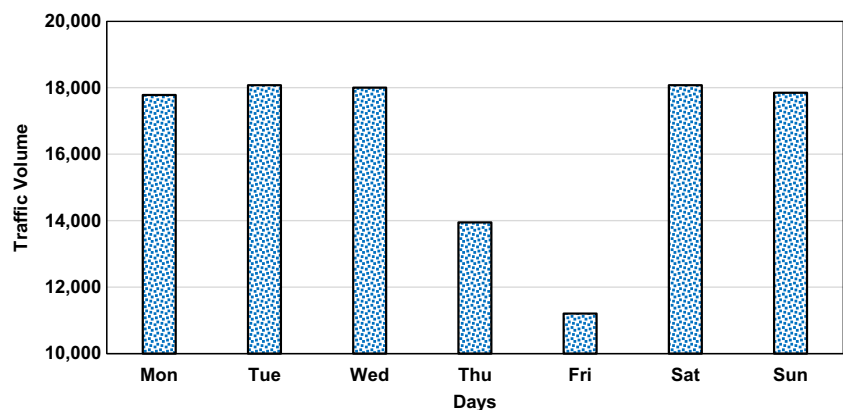
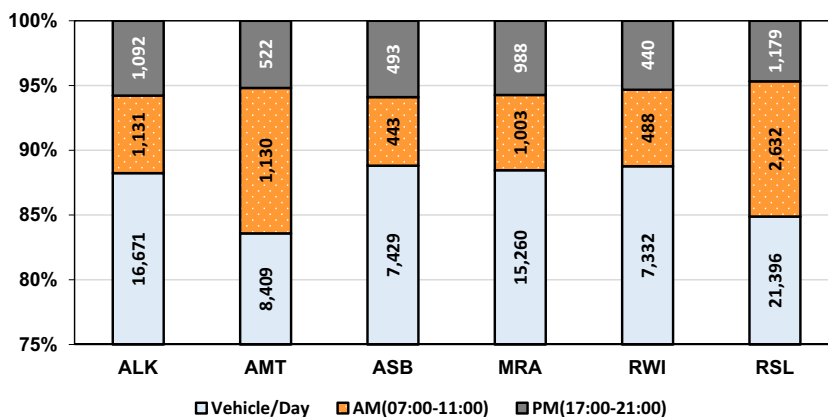


Fig. 3 The average daily traffic and peak volumes (AM-PM) of the six modeling locations on weekdays



Recordum-GmbH, Austria) and an ETL3000 station (UniTec, Italy) based on European Union (EU) and US EPA directives (Pelletier et al. 2017; Weichenthal et al. 2015). CO was measured through non-dispersive infrared (NDIR) filter gas correlation procedure with a lower detection limit of 0.04 ppm and a precision of ±0.1 ppm. NOx data were collected via chemiluminescence method. The NOx detection limits and precision levels were 0.4 ppb and < 500 ppb ± 1% of reading > 100 ppm, respectively. In addition, hourly ambient temperature, pressure, and wind speed were measured at each location with an integrated meteorological station installed on the instruments. These meteorological data were applied for the simulation of the vehicle emission rates at each study location.

Quality assurance

Measurements were taken for 24 h for each of the six monitoring locations within January–December 2018 for both summer and winter seasons. The instruments were placed at a distance of 6.6–11 m away from the roads during the entire

monitoring period. The maximum optimal temperature (+ 40 °C) for operations of the instruments was maintained. Calibrations including regular changes/cleaning of adsorbents were performed while ensuring zero in-built span gas in the instrument. After spending 1440 min of sampling from each location, the measured traffic data across the six locations were visually assessed for possible outliers and other data gaps (< 1% of the total measured data).

Emission modeling

US EPA (2018b) recommends that receptors should be placed at least 5 m or 25 m closer to the road source and later wider spacing of at least 100 m further away from the road sources. Following Liu et al. (2019) approach, high-resolution receptors from 5 to 100 m at 15 m intervals closer to the road source and later 50 m interval from 100 to 200 m further away from the road source were used for each of the modeling locations. Finally, the hourly (HH:MM) concentration of CO and NOx

Fig. 4 Average vehicle classification by volumes in six modeling locations in Muscat

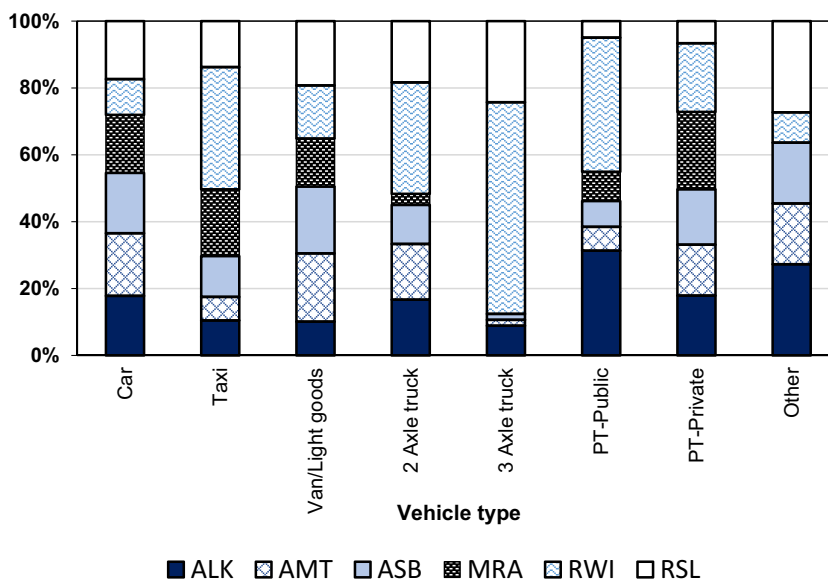


Table 1 Fleet composition and input environmental data for CMEM model

Modeled location	Fleet composition (%)		Air pressure (kPa)	Ambient temperature (°C)	Velocity (kph)
	LDV	HDV			
ALK	97.0	3.0	101.04	24.0	0.8
AMT	99.0	1.0	99.30	35.0	3.9
ASB	99.0	1.0	101.37	25.6	2.1
MRA	99.9	0.1	99.32	35.7	2.6
RWI	85.0	15.0	100.40	33.5	2.3
RSL	95.0	5.0	100.40	24.7	1.1

were predicted by the AERMOD from 00:00 to 23:00 for each road across the six locations.

CMEM model

CMEM model was used to calculate emission factors (g/veh km) for CO and NOx emitted from on-road vehicles in Muscat. CMEM is a microscopic traffic model developed by Centre for Environmental Research and Technology (<https://www.cert.ucr.edu/cmem/>) at the University of California-Riverside, USA. The microscopic nature of CMEM enables simulation of second-by-second tailpipe pollutants and fuel consumption rates for a wide range of vehicle types/technologies for operating conditions such as properly functioning, deteriorating, and malfunctioning states of the vehicles (Zhang and Ioannou 2016). CMEM was selected for the study because it is less data-driven and incorporate local meteorological data compared to other models such as US EPA’s MOVES model and Mobile Source Emission Factor Model (MOBILE6). In order to run the CMEM model,

traffic microsimulation model (VISSIM) output of second-by-second velocity and acceleration rate data are required (Abou-Senna et al. 2013). Due to the lack of such data in Muscat road network, the default VISSIM data for this study was employed. Also, default data on model calibration parameters such as fuel, soak time, hot catalyst, and engine out-pollutant emission-coefficient values were used. Additionally, the proportion of fleet volumes defined as LDV and HDV from each of the study location was used as input parameter into the model. Further, location-specific meteorological data on ambient temperature, pressure, and wind speed were incorporated. Table 1 indicates the fleet data and environmental parameters used for the CMEM model. Employing local meteorological data in this study is crucial in predicting locally based emission factors due to harsh environmental conditions in Muscat. The CMEM emission factors were converted into emission rates as required by the dispersion model based on total vehicle population (Fig. 2). The roadway coordinates and the total area of each location (Table 3) were assumed according to the method used by Charabi et al. (2018) and Abdul-

Table 2 Surface and upper air meteorological information used for the air dispersion modeling acquired from Muscat International Airport

Parameters	Surface air (min–max value)	Upper air (min–max value)
(A) Meteorological factors:		
Temperature (K)	287–319	13.9–99.9
Relative humidity (%)	6.0–100	NA
Wind speed (m/s)	0.0–16.5	0–999
Wind direction (°)	0.0–360	0–360
Mechanical mixing height (m)	19–3723	NA
Convective mixing height (m)	3.0–4000	NA
Sensible heat flux (W/m ²)	–64–296	NA
Friction velocity (m/s)	0.032–1.340	NA
(B) Land use parameters:		
Albedo	0.18–1.0	NA
Bowen ratio	0.96–0.98	NA
Surface roughness (m)	0.013–0.123	NA

NA non-applicable

Table 3 The road and terrain parameters of the selected locations

Location	Roadway coordinates (UTM: x, y) m		Base elevation (m)	Total area (m ²)	Road area (m ²)	AQM date (2018)	Site type	AQM distance from road (m)
	Start	End						
ALK	646,950.15, 2,610,136.52	646,297.23, 2,610,145.36	18.28	1.0516×10^7	1.6×10^4	28/01	Urban	10.5
AMT	652,393.07, 2,596,070.52	651,982.66, 2,596,263.38	132.58	2.7225×10^8	7.0×10^3	03/05	Suburban	6.6
ASB	621,505.82, 2,618,772.92	621,048.88, 2,619,288.77	6.40	3.7199×10^7	3.0×10^4	02/03	Urban	11.0
MRA	661,968.88, 2,612,663.38	661,780.44, 2,612,950.37	10.36	8.4652×10^5	4.0×10^3	10/06	Suburban	4.7
RWI	657,556.33, 2,610,170.48	658,133.05, 2,610,404.49	39.01	2.6151×10^6	9.0×10^3	07/09	Urban	7.0
RSL	624,152.65, 2,606,164.73	623,305.65, 2,606,452.69	78.02	6.8271×10^6	1.2×10^4	08/12	Industrial	10.0

Wahab and Fadlallah (2014). Table 4 shows the final emission rate values for the dispersion model for all the six modeling locations.

COPERT IV emission data

The study also aimed at comparing emissions from CMEM modeling outputs with COPERT IV emission factor data to understand which of these emission factors perform well with traffic emissions in Muscat. Therefore, COPERT IV emission factor data (g/veh km) of CO and NO_x were obtained from National Atmospheric Emission Inventory data available at <http://naei.beis.gov.uk/data/ef-transport>. Here, the emission factors were developed based on fleet composition, weight emission standards, vehicle specifications, abatement technologies, fuel types, temperature conditions, and driving behaviors. Table 5 provides a summary of emission factors and their associated process for CO and NO_x. Air dispersion emission rates (g/m²/s) were estimated by considering the COPERT IV emission factors and average speed of 30 km/h (Table 5), total vehicle volumes (Fig. 2), and the area of the road (Table 3) for each of the six roads in Muscat (Abdul-

Wahab and Fadlallah 2014). Table 6 lists the calculated emission rates for each location for air dispersion modeling study.

Air dispersion modeling

The individual roads in Muscat were modeled with US EPA Line source tool of the AERMOD dispersion model. The detailed description of the AERMOD model is available at Amoatey et al. (2018a). The emission rates (g/m²/s) from CMEM and COPERT IV data were applied to the model to estimate the near-road dispersion of CO and NO_x. The start and end UTM coordinates (m) of each road, release height, and the initial vertical dimension (σ_{z_0}) were calculated by dividing the effective height by 2.15 (Thus, the point of release of the pollutants should be 2.15 times the vertical dimension, σ_{z_0}) as shown in Table 3 and Table 7, respectively (US EPA 2018b). All these data were used as an input parameter of the US EPA Line source in AERMOD (Abdul-Wahab and Fadlallah 2014; US EPA 2018b). Here, the line source uses the area source algorithm with the assumption that the traffic emissions (g/m²/s) are uniformly dispersed across the dimensions of the line sources. Also, the model does not simulate the horizontal meander component of the pollutant dispersion

Table 4 Emission rates for CO and NO_x based on CMEM model

Location	Emission factors (g/veh km)		Emission rates (g/s)		Emission rates (g/m ² /s)	
	CO	NO _x	CO	NO _x	CO	NO _x
ALK	20.225	12.582	2809.75	1747.95	2.6716×10^{-4}	1.6620×10^{-4}
AMT	17.106	4.466	1198.70	312.95	4.4028×10^{-6}	1.1494×10^{-6}
ASB	17.11	4.476	1059.25	277.10	2.8474×10^{-5}	7.4489×10^{-6}
MRA	15.708	0.825	1997.53	104.91	2.3596×10^{-3}	1.2392×10^{-4}
RWI	38.873	61.125	2375.14	3734.73	9.0823×10^{-4}	1.4281×10^{-3}
RSL	23.337	20.681	4160.98	3687.42	6.0947×10^{-4}	5.4011×10^{-4}

Table 5 COPERT IV road transport emission factors (NAEI 2019)

Pollutant	Emission processes	Average speed (km/h)	Emission factors (g/veh km)
NOx	Hot exhaust emissions and cold start exhaust emissions	30	0.820
CO		30	0.358

compared to point and volume sources. Thus, the line source is used to predict concentrations of the pollutants located within the dimension of the source (US EPA 2018b). There is no reliable background concentration data available for these sites for years preceding this study, thereby the lowest recorded concentration value was utilized as background concentration in each site.

Model evaluation

The performance of the AERMOD (US EPA Line source) model was determined by comparing the predicted values of hourly CO and NOx concentrations with the observed values from 00:00 to 23:00 for January–December 2018 for each of the six locations. These evaluations were conducted by using US EPA recommended air quality statistical models (Mohan et al. 2011). These statistical performance measures have been previously applied as common framework for European Union Initiative on “Harmonizing within the Atmospheric Dispersion Modeling for Regulatory Purposes” (Cai and Xie 2011). To achieve the model evaluation, three linear statistical measures including fractional bias (FB), normalized mean square error (NMSE), and correlation coefficient (R) were considered. The FB and NMSE are both quantitative statistical models used to determine over-/underprediction and accuracy of the model performance, respectively, whereas qualitative statistical measures (R) determine the association between the modeled and the observed results. Geometric mean bias (MG) and geometric variance (VG) performance measures were also employed to account for a more balanced treatment of extremely high and low predicted values based on logarithm transformation, of which FB and NMSE cannot do. In addition, bootstrap resampling statistical technique was used to

estimate the confidence interval (CI) at 95% using NMSE, FB, and R performance measures for COPERT and CMEM models. This is because they are deemed as the most basic statistical measures, and they are more suitable for mid-range model output pollutant concentrations to evaluate air quality models (Kadiyala and Kumar 2012). This analysis will help to establish whether the performance of COPERT and CMEM model outputs are statistically different from 0 at 95% CI compared with observed data or not. In this study, all the primary and bootstrap resampling analysis were performed through Microsoft Excel® (Version 2016) and BOOT® Software (version 2.01), respectively. All the statistical performance measures are presented by Eqs. 1–5 below.

$$FB = \frac{\bar{C}_o - \bar{C}_p}{0.5 \left(C_o + C_p \right)} \tag{1}$$

$$NMSE = \frac{(C_o - C_p)^2}{(C_o C_p)} \tag{2}$$

$$R = \frac{(C_o - C_o) (C_p - C_p)}{\sigma_{C_o} \sigma_{C_p}} \tag{3}$$

$$MG = \exp(\overline{\ln C_o} - \overline{\ln C_p}) \tag{4}$$

$$VG = \exp \left[\left(\overline{\ln C_o} - \overline{\ln C_p} \right)^2 \right] \tag{5}$$

The symbols Cp, Co, C, σ and ln denote the predicted concentration, the observed concentration, the average of the

Table 6 Modeled location-specific emission rates estimations based on COPERT IV data

Location	Daily vehicle volume (Veh.)	Emission rates (g/s)		Emission rates (g/m ² /s)	
		NOx	CO	NOx	CO
ALK	16,671	113.918	49.735	7.1198 × 10 ⁻³	3.1084 × 10 ⁻³
AMT	8409	57.461	25.086	8.2087 × 10 ⁻³	3.5837 × 10 ⁻³
ASB	7429	50.764	22.163	1.6921 × 10 ⁻³	7.3876 × 10 ⁻⁴
MRA	15,260	104.276	45.525	2.6069 × 10 ⁻²	1.1381 × 10 ⁻²
RWI	7332	50.102	21.873	5.5668 × 10 ⁻³	2.4303 × 10 ⁻³
RSL	21,396	146.206	63.831	1.2183 × 10 ⁻²	5.3192 × 10 ⁻³

Table 7 AERMOD EPA Line source input parameters for the modeled locations

Parameter	Value (m)
Released height	0.35
Initial vertical dimension, σ_{z0}	0.2
Road width	10

concentrations, the standard deviation, and the natural logarithm, respectively. Figure 5 illustrates a flowchart describing the steps of the entire modeling study in “Data and methods.”

Results and discussion

The COPERT IV emission data and the estimated CMEM emission rates were employed as input for EPA Line source of the AERMOD dispersion modeling system in prediction of CO and NO_x. Also, the measured concentrations and allowable threshold limits of the pollutants are presented and compared with the predicted concentrations for the six roads located in ALK, AMT, ASB, MRA, RWI, and RSL. The analysis of the results consists of three components, including CO concentrations, NO_x concentrations, and model evaluation.

CO concentrations

By selecting CO as a case study, distinctive predicted concentrations for COPERT IV and CMEM emission rates input data were obtained. Table 8 presents the top five maximum hourly concentrations of CO for the three main traffic rush hours in Muscat defined as morning (6:00 and 8:00), afternoon (13:00), and evening (20:00 and 22:00) peak hours along with the near-road locations. It can be seen that although the model predicted higher concentrations of CO for COPERT IV input data compared to CMEM across all the six roads, most of the predicted concentrations were within the US EPA standard

(40,096.1 $\mu\text{g}/\text{m}^3$). However, MRA experienced two highest predicted concentrations during the time 20:00 (83,038.83 $\mu\text{g}/\text{m}^3$) and 22:00 (55,695.54 $\mu\text{g}/\text{m}^3$), thereby exceeding the US EPA’s allowable limit. Similarly, slightly higher prediction of 41,455.64 $\mu\text{g}/\text{m}^3$ than the US EPA limit also occurred in AMT during the 22:00 period.

Moving to the measured concentrations of CO, they were also found below the US EPA standards similar to most of the model concentrations. However, higher concentrations were measured for all the three peak hours in MRA and AMT exceeding an average of 10,000 $\mu\text{g}/\text{m}^3$ compared to the remaining locations. Figure 6 shows a time-series concentrations levels of CO for each location measured over 24 h. Interestingly, the results from this study showed consistency in trends for higher concentration levels of CO for both the predicted and the measured values in these two locations (MRA and AMT) (Table 8). The similarities in the concentrations of these two locations may be attributed to the influence of meteorological factors due to its proximity to the sea (Sultan Qaboos Port) and mountainous terrain features compared to the other roads (Abdul-Wahab and Fadlallah 2014). Also, the measured and predicted concentrations may not be due to poor dispersal of the CO emissions as these locations are characterized by several mountains (Zhang et al. 2019). In general, visual comparison of all the predicted and the measured concentrations showed increased in CO levels during the morning where traffic was at the peak and decreased when traffic volumes reduce and later increased again during evening hours. Thus, these variations in CO concentrations may be highly dependent on traffic emissions.

NO_x concentrations

For the emissions of NO_x, Table 9 shows the AERMOD predicted concentrations of COPERT IV and CMEM emission rate input parameters for the six modeled locations in Muscat. The predicted concentrations were visually compared with the measured and the allowable limit established by the

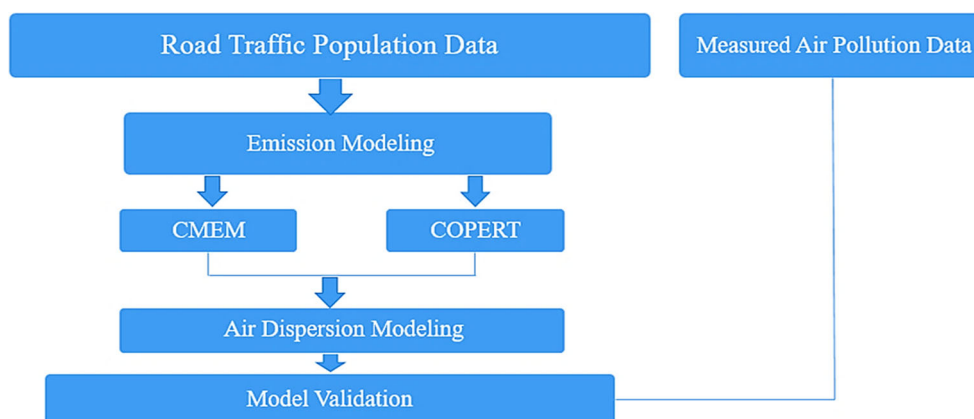
Fig. 5 Full-chain road traffic modeling processes of Muscat

Table 8 Comparison of top 5 peaks modeled AERMOD values from COPERT IV and CMEM input values with observed concentrations of CO among the six modeled locations in Muscat from 00:00 to 23:00

Location (date)	Time (HH:MM)	Modeled value ($\mu\text{g}/\text{m}^3$)		Observed value ($\mu\text{g}/\text{m}^3$)	1-hr threshold average concentration
		COPERT IV	CMEM		
ALK 28/01/2018	06:00	39,044.75	3355.80	2360	40,096.1 $\mu\text{g}/\text{m}^3$ (35 ppm) CO
	08:00	6326.00	543.70	5950	
	13:00	5152.42	442.83	2540	
	20:00	12,166.13	1045.65	4100	
	22:00	16,872.41	1450.14	3210	
AMT 03/05/2018	06:00	14,135.60	17.36	13,440	
	08:00	5787.43	7.11	14,540	
	13:00	3453.55	4.24	12,460	
	20:00	25,676.66	31.54	12,790	
	22:00	41,455.64	50.93	15,220	
ASB 02/03/2018	06:00	3060.44	117.95	4400	
	08:00	1246.17	48.03	4690	
	13:00	1198.45	46.19	4450	
	20:00	3069.51	118.30	4810	
	22:00	2832.20	109.16	5370	
MRA 10/06/2018	06:00	45,107.17	9351.98	15,980	40,096.1 $\mu\text{g}/\text{m}^3$ (35 ppm) CO
	08:00	22,090.87	4580.05	16,140	
	13:00	20,949.65	4343.44	16,360	
	20:00	83,038.83	17,216.27	16,340	
	22:00	55,695.54	11,547.24	16,980	
RWI 07/09/2018	06:00	16,965.72	6340.28	610	
	08:00	7347.08	2745.68	540	
	13:00	1702.02	636.06	1030	
	20:00	28,181.14	10,531.60	2850	
	22:00	15,776.43	5895.82	3350	
RSL 08/12/2018	06:00	20,434.94	2341.42	2900	
	08:00	18,469.70	2116.24	1200	
	13:00	8829.61	1011.69	900	
	20:00	25,035.84	2868.58	1600	
	22:00	21,179.93	3383.87	2100	

US EPA threshold limit of $188.2 \mu\text{g}/\text{m}^3$ for NO_2 since, currently, there is no criterion set for NO_x emissions (US EPA 2018c). It could be observed from Table 9 that the two emission rate data of the model predicted maximum hourly NO_x concentrations of about 10–100 folds higher than the observed concentrations. The model prediction based on CMEM emission data for AMT and ASB was found very low, thereby meeting the US EPA standard of $188.2 \mu\text{g}/\text{m}^3$ for NO_2 . Despite the high predictions made by the model in certain hours of the day, there were a similar pattern in terms of increase, decrease, and increase in NO_x concentration levels with respect to morning (6:00 and 8:00), afternoon (13:00), and evening (20:00 and 22:00) peak hours across all the model locations, respectively. For example, in ALK, the model predicted high NO_x levels at 6:00 to be $2087 \mu\text{g}/\text{m}^3$ which later

decreased drastically to $275 \mu\text{g}/\text{m}^3$ at 13:00 increased again to $902 \mu\text{g}/\text{m}^3$ during the peak hour of 22:00 based on the CMEM emission data. Similar to COPERT IV data, the model predicted concentrations of $89,432 \mu\text{g}/\text{m}^3$, $11,801 \mu\text{g}/\text{m}^3$, and $38,646 \mu\text{g}/\text{m}^3$ during the same three peak hours of the day as described above. The high predictions of COPERT compared to CMEM could be due to the utilization of local or location-specific traffic and meteorological data during CMEM emission rates estimation, whereas such local data was lacking in COPERT. These variations in the predicted concentrations attest that the NO_x levels were primarily attributed to traffic emissions. Also, the road traffic NO_x concentration levels were found to be very low with average hourly concentrations (22 to $160 \mu\text{g}/\text{m}^3$) among the six roads. Figure 6 also shows detailed time-series NO_x concentrations

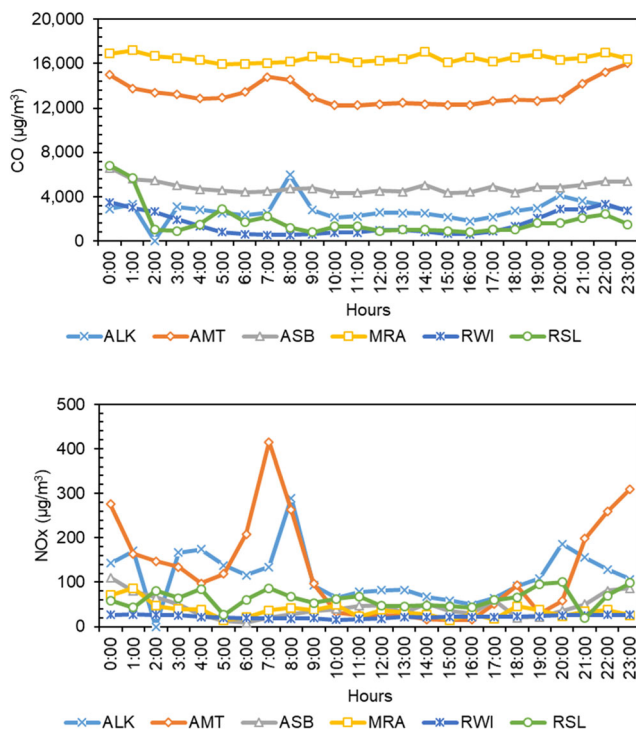


Fig. 6 Average measured hourly concentrations of CO (top) and NO_x (bottom) from each modeling location

measured from each location over 24-h durations. These measured values were found to be very low compared to the predicted concentrations (Table 9), which could be due to rapid transformation of the NO_x to O₃ through photochemical reactions as solar radiation levels are generally high in Muscat (Agudelo-Castaneda et al. 2014; Directorate General of Meteorology 2019). This low model prediction levels were also evidenced by the lower measured NO_x levels (Table 9). According to Amoatey et al. (2019), nitric oxide (NO) is very unstable gas and is the major component of NO_x (95% vol. NO_x) when emitted from vehicular tailpipes. These imply that most of the NO_x might have been converted to an unstable NO thereby decreasing the measured and the predicted concentration levels across the modeled locations. Thus, it is imported to incorporate NO_x (NO₂–NO–O₃) chemical transformation algorithms into future traffic modeling studies in order to improve the accuracy of the predicted concentrations levels (Halonen et al. 2016).

Model evaluation

The statistical performance measure outputs for the measured and predicted concentrations across the six locations are summarized in Table 10. In overall, the statistical models predicted the concentrations of CO and NO_x moderately well and poor for certain locations. In ASB, FB model revealed moderate propensity of AERMOD to underestimate NO_x (FB = 0.39) and CO (FB = 0.47) concentration levels for CMEM and

COPERT IV input data, respectively. However, FB showed a low tendency for the COPERT IV model to over-predict CO (FB = −0.23) in AMT. For the performance measures, there was satisfactory model performance based on NMSE statistics in ASB for CO = 0.44 and NO_x = 0.5 for COPERT IV and CMEM input parameters, respectively. However, as shown in Table 10, NMSE results for CO in AMT (0.95) and MRA (0.69) were found to be moderate. The above model performances of FB and NMSE were based on the criteria used by the study conducted by Mohan et al. (2011); thus, a model prediction is deemed acceptable if $-0.5 < FB < +0.5$ and $NMSE < 0.5$.

It is very clear that very few locations had moderate prediction and performance while the majority showed very poor over-prediction and performances with the measured results (Table 10). Regarding the relationship between the modeled and measured pollutants, the association (R) were found to be moderate in all the locations for CO (0.51–0.64), with an exception of MRA (R = 0.25), which showed a weak correlation. For NO_x, very good correlation was found in ALK (R = 0.70), while moderate association were found in AMT (R = 0.50) and RSL (R = 0.49). The detailed statistical associations between the predicted model results based on COPERT IV and CMEM input data and the observed concentrations in each location are shown in Table 10. In addition, due to the varying (extremely low and high values) predicted concentration levels of both COPERT and CMEM outputs, MG and VG performance measures were utilized to evaluate these predicted concentrations based on a logarithmic scale (Table 11). According to the standard model acceptance criteria range for MG (0.70–1.30) and VG (1.50–4.00) suggested by Chang and Hanna (2004), the model performance for the current study seems moderate; however, several locations could not meet the above performance. For example, COPERT IV showed good performance for CO (MG = 1.07) in AMT. For the same model, the VG statistical measure for several roads including ASB (2.33), MRA (2.75), and AMT (2.00) had predicted CO levels within the above model acceptance criteria. In the case of CMEM model, a similar situation was also found in RSL where the estimated VG = 1.91 satisfied the acceptable limits for CO. As indicated in Table 11, the model evaluation showed weak performance towards NO_x. For example among all the location, only ASB (VG = 2.32) satisfied the performance measure for CMEM model. It should be noted that, in a more stringent model acceptability criteria, both COPERT IV and CMEM models will show poor performance (Amoatey et al. 2018a; Kumar et al. 1992).

Tables 12 and 13 indicate detailed 95% CI estimates over NMSE, FB, and R obtained from bootstrap resampling analysis for both individual models (COPERT and CMEM) and between models for CO and NO_x (Kumar et al. 2012). In ALK, the bootstrap 95% CI estimates over NMSE and FB for CO were statistically different from 0 (the signs for lower

Table 9 Comparison of top 5 peaks modeled AERMOD values from COPERT IV and CMEM input values with observed concentrations of NOx among the six modeled locations in Muscat from 00:00 to 23:00

Location (date)	Time (HH:MM)	Modeled value ($\mu\text{g}/\text{m}^3$)		Observed value ($\mu\text{g}/\text{m}^3$)	1-h threshold average concentration
		COPERT IV	CMEM		
ALK 28/01/2018	06:00	89,432.14	2087.64	116.21	188.2 $\mu\text{g}/\text{m}^3$ (100 ppb), NO ₂
	08:00	14,489.73	338.239	289.05	
	13:00	11,801.65	275.49	83.13	
	20:00	27,866.56	650.49	185.96	
	22:00	38,646.31	902.13	128.62	
AMT 03/05/2018	06:00	32,378.52	4.53	207.95	
	08:00	13,256.49	1.85	262.76	
	13:00	7910.60	1.11	23.55	
	20:00	58,814.06	8.23	57.48	
	22:00	94,956.80	13.29	258.9	
ASB 02/03/2018	06:00	70,09.82	30.85	9.11	
	08:00	2854.31	12.56	26.95	
	13:00	2745.01	12.08	32.10	
	20:00	7030.60	30.94	35.71	
	22:00	6487.04	28.55	81.21	
MRA 10/06/2018	06:00	103,321.23	491.14	20.39	188.2 $\mu\text{g}/\text{m}^3$ (100 ppb), NO ₂
	08:00	50,600.73	240.53	41.73	
	13:00	47,986.69	228.11	32.06	
	20:00	190,206.42	904.15	23.9	
	22:00	127,574.64	606.43	37.09	
RWI 07/08/2018	06:00	38,861.38	9969.45	18.52	
	08:00	16,829.10	4317.31	18.08	
	13:00	3898.63	1000.15	21.79	
	20:00	64,551.20	16,559.88	25.49	
	22:00	36,137.21	9270.59	26.45	
RSL 08/12/2018	06:00	46,803.84	2074.95	26.6	
	08:00	42,302.67	1875.40	66.7	
	13:00	20,223.18	896.55	46.5	
	20:00	57,341.63	2542.13	95.4	
	22:00	67,642.02	2998.77	19.2	

and upper limits did not change) for the individual model comparison except for R (due to change in signs for the CI limits) in CMEM model (Table 12). Intra-model (combined) comparison also indicated statistical significance for all the performance measures for both COPERT and CMEM models as listed in Table 13. A similar situation was also recorded for NOx where individual model 95% CI estimates over NMSE and FB were found not to be statistically different from 0 with the exception of R for both models. However, all the performance measures (NMSE, FB, and R) were statistically different from 0 between model comparisons. Also in AMT, the individual comparison for CO showed that all the measures were not statistically different from 0 except NMSE for NOx; however, both NMSE and FB were found to be statistically

different from 0 (Table 12). Interestingly, comparison of CO and NOx was significantly different from 0 between COPERT and CMEM models (Table 13).

Interestingly, in ASB, both CO and NOx bootstrap 95% CI estimates for all the measures were statistically different from 0 for both individual models and between model performances with the exception of R for NOx which was not statistically different from 0 for individual model performance. The study found an interesting model performance evaluations in RWI, where all the pollutants (CO and NOx) showed statistical significance (at 95% CI) for both the individual models (COPERT and CMEM) and between model comparison (Tables 12 and 13). Also for individual model performance comparison, the bootstrap 95% CI estimates over

Table 10 Linear performance measures of AERMOD predictions based on COPERT IV and CMEM input values and the measured concentrations across the six locations

Locations	FB (CMEM)		FB (COPERT IV)		NMSE (CMEM)		NMSE (COPERT IV)		R (CMEM and COPERT IV)			
	CO	NOx	CO	NOx	CO	NOx	CO	NOx	CO	P value	NOx	P value
ALK	1.41	-1.46	-1.34	-1.98	<i>1.05</i>	<i>6.89</i>	5.74	371.89	<i>0.53</i>	0.01	<i>0.7</i>	0.0002
AMT	1.99	1.83	-0.23	-1.98	629.17	33.28	<i>0.95</i>	496.65	<i>0.59</i>	0.0027	<i>0.5</i>	0.0128
ASB	1.90	<i>0.39</i>	<i>0.47</i>	-1.97	38.28	<i>0.50</i>	<i>0.44</i>	205.37	<i>0.51</i>	0.0116	0.15	0.4652
MRA	<i>0.55</i>	-1.72	-0.92	-1.99	<i>0.72</i>	17.18	<i>0.69</i>	4015.97	0.25	0.2403	-0.07	0.7162
RWI	-1.08	-1.98	-1.59	-1.99	3.17	656.78	11.10	2565.96	<i>0.64</i>	0.0033	0.39	0.0913
RSL	-0.60	-1.91	-1.76	-1.99	1.46	62.34	21.67	1448.83	<i>0.56</i>	0.0047	<i>0.49</i>	0.0144

Perfect model estimation, performance, and association should have FB, NMSE, and R values to be 0, 0, and 1, respectively (Cai and Xie 2011)
 The *italicized* values meet the minimum criteria of the individual statistical performance measures

NMSE and FB were statistically different from 0 for CO and NOx for all the models in MRA, whereas R was not found significantly different from 0. Similar performance was also observed in RSL for CO and NOx for the individual COPERT and CMEM model comparison except for NMSE (in CMEM model), which was not statistically different from 0 (Table 13). Finally, the bootstrap 95% CI estimates for the combined model comparison of CO and NOx for both MRA and RSL were found statistically significant from 0 (Table 13).

In terms of modeling study, the study faced several limitations including the inability of the EPA line source to simulate vertical dispersion of the pollutants but rather considers the horizontal distribution of the pollutants long the road, which could lead to over prediction and underestimation of the predicted pollutants. Also, the lack of background data for CO and NOx in close proximity to the modeled locations could be a major factor in the overall performance of the model predictions. Khreis et al. (2018) found that incorporating background NOx concentrations (ranging from 8.5 to 71 µg/m³) other than road sources could enhance the performance of the model. In addition, most roads have planted

green vegetation (mainly turf grass) and these turf grasses near the roads are frequently managed through mowing activities (Amoatey et al. 2018b). Thus, the emission from the mowers could be the major contributor to background CO and NOx concentrations.

Although the study estimated emission rates of CO and NOx with CMEM model by using road-specific meteorological factors and the proportion of LDV and HDV for each road, there was a lack of second-by-second vehicle velocity and acceleration data, vehicle engine emission data, as well as the most recent traffic data. All these factors affected the CMEM emission rate data and the performance of the model with respect to measured values. Thus, in order to ensure accurate prediction of traffic emissions from roads in Oman, it is crucial to develop a local emission rate data and air dispersion modeling system since Oman has different meteorological and terrain features compared to developed countries where these models were adapted from.

Despite the limitations, this study provides very useful datasets about the road traffic emission modeling in Muscat and many arid countries compared to previous studies (Abdul-Wahab and Fadlallah 2014). This is the first study where US

Table 11 Logarithmic performance measures of AERMOD predictions based on COPERT IV and CMEM input values and the measured concentrations across the six locations

Locations	MG (CMEM)		MG (COPERT IV)		VG (CMEM)		VG (COPERT IV)	
	CO	NOx	CO	NOx	CO	NOx	CO	NOx
ALK	2.77	0.17	0.24	0.005	4.28	27.41	11.86	1.7E13
AMT	874.9	20.31	<i>1.07</i>	0.003	3426.8	2.1E4	<i>2.00</i>	2.1E15
ASB	52.35	<i>1.57</i>	<i>2.01</i>	0.006	9.1E6	2.32	2.33	1.0E11
MRA	2.23	0.08	<i>0.46</i>	0.0004	2.92	819.8	2.75	6.3E26
RWI	0.38	0.0043	0.14	0.0011	4.62	1.9E13	78.3	3.2E20
RSL	<i>0.60</i>	0.027	0.069	0.0012	<i>1.91</i>	6.1E5	1854.6	4.9E19

MG and VG should be equal to 1 to deem the model as perfect one

The *italicized* values meet the minimum criteria of the individual statistical performance measures

Table 12 Inter-model (individual models) comparison using bootstrap CI 95% estimates over NMSE, FB, and R for CO and NOx

Locations	Models	Measures	Lower limits	Upper limits	Student's <i>t</i> test	Mean	SD	
Student's <i>t</i> test at 95% CI for CO								
ALK	COPERT	NMSE	3.371	8.15	4.999	5.76	1.152	
		FB	- 1.512	- 1.158	- 15.621	- 1.335	0.085	
		R	0.326	0.699	0.756	0.187	0.247	
	CMEM	NMSE	0.277	1.961	2.756	1.119	0.406	
		FB	0.523	1.047	6.217	0.785	0.126	
		<i>R</i>	- 0.326	0.699	0.756	0.187	0.247	
	AMT	COPERT	NMSE	0.461	1.405	4.092	0.933	0.228
			<i>FB</i>	- 0.581	0.051	- 1.738	- 0.265	0.153
			<i>R</i>	- 0.042	0.806	1.866	0.382	0.205
CMEM		NMSE	420.739	842.592	6.196	631.666	101.946	
		FB	***	***	***	1.994	0.000	
		<i>R</i>	- 0.042	0.806	1.866	0.382	0.205	
ASB		COPERT	NMSE	0.234	0.759	3.915	0.497	0.127
			FB	0.234	0.743	3.969	0.488	0.123
			R	0.115	1.004	2.602	0.559	0.215
	CMEM	NMSE	29.707	53.432	7.251	41.569	5.733	
		FB	1.884	1.932	163.471	1.908	0.012	
		R	0.115	1.004	2.602	0.559	0.215	
	MRA	COPERT	NMSE	1.291	4.08	3.985	2.686	0.674
			FB	- 1.177	- 0.668	- 7.51	- 0.923	0.123
			<i>R</i>	- 0.279	0.544	0.664	0.132	0.199
CMEM		NMSE	0.352	1.011	4.285	0.681	0.159	
		FB	0.258	0.846	3.888	0.552	0.142	
		<i>R</i>	- 0.279	0.544	0.664	0.132	0.199	
RWI		COPERT	NMSE	7.457	20.702	4.399	14.079	3.201
			FB	- 1.716	- 1.468	- 26.556	- 1.592	0.06
			R	0.261	0.856	3.883	0.558	0.144
	CMEM	NMSE	1.59	6.345	3.453	3.968	1.149	
		FB	- 1.31	- 0.83	- 9.232	- 1.07	0.116	
		R	0.261	0.856	3.883	0.558	0.144	
	RSL	COPERT	NMSE	8.956	40.421	3.297	24.688	7.488
			FB	- 1.861	- 1.663	- 37.461	- 1.762	0.047
			<i>R</i>	- 0.097	0.764	1.629	0.334	0.205
CMEM		NMSE	- 0.057	3.192	2.027	1.568	0.773	
		FB	- 0.991	- 0.186	- 3.072	- 0.588	0.192	
		<i>R</i>	- 0.097	0.764	1.629	0.334	0.205	
Student's <i>t</i> test at 95% CI for NOx								
ALK		COPERT	NMSE	278.251	553.362	6.269	415.806	66.324
			FB	- 1.992	- 1.979	- 622.534	- 1.986	0.003
	<i>R</i>		- 0.043	0.971	1.898	0.464	0.244	
	CMEM	NMSE	4.661	10.705	5.273	7.683	1.457	
		FB	- 1.605	- 1.321	- 21.327	- 1.463	0.069	
		<i>R</i>	- 0.043	0.971	1.898	0.464	0.244	
	AMT	COPERT	NMSE	299.343	769.939	4.701	534.641	113.726
			FB	- 1.992	- 1.983	- 939.475	- 1.987	0.002
			<i>R</i>	- 0.184	0.707	1.214	0.262	0.215
CMEM		NMSE	20.078	54.786	4.463	37.432	8.388	
		FB	1.767	1.89	61.624	1.829	0.03	

Table 12 (continued)

		<i>R</i>	<i>- 0.184</i>	<i>0.707</i>	<i>1.214</i>	<i>0.262</i>	<i>0.215</i>
ASB	COPERT	NMSE	150.278	295.292	6.357	222.785	35.044
		FB	- 1.981	- 1.966	- 541.786	- 1.973	0.004
		<i>R</i>	<i>- 0.145</i>	<i>0.837</i>	<i>1.457</i>	<i>0.346</i>	<i>0.237</i>
	CMEM	NMSE	0.326	1.045	3.945	0.686	0.174
		FB	0.107	0.692	2.822	0.399	0.141
		<i>R</i>	<i>- 0.145</i>	<i>0.837</i>	<i>1.457</i>	<i>0.346</i>	<i>0.237</i>
MRA	COPERT	NMSE	2933.68	6176.396	5.813	4555.038	61.955
		FB	- 2.003	- 1.994	- 872.168	- 1.999	0.002
		<i>R</i>	<i>- 0.544</i>	<i>0.667</i>	<i>0.209</i>	<i>0.061</i>	<i>0.293</i>
	CMEM	NMSE	12.133	27.257	5.389	19.695	3.655
		FB	- 1.813	- 1.636	- 40.525	- 1.725	0.043
		<i>R</i>	<i>- 0.544</i>	<i>0.667</i>	<i>0.209</i>	<i>0.061</i>	<i>0.293</i>
RWI	COPERT	NMSE	1743.031	3516.847	6.135	2629.939	23.861
		FB	- 2.001	- 1.993	***	- 1.997	0.002
		<i>R</i>	0.201	0.738	3.616	0.47	0.13
	Model-B	NMSE	445.567	900.634	6.121	673.101	109.973
		FB	- 1.991	- 1.987	***	- 1.989	0.001
		<i>R</i>	0.201	0.738	3.616	0.47	0.13
RSL	COPERT	NMSE	940.886	2240.705	5.143	1590.796	90.101
		FB	- 2.002	- 1.99	- 677.168	- 1.996	0.003
		<i>R</i>	<i>- 0.003</i>	<i>0.872</i>	<i>2.086</i>	<i>0.435</i>	<i>0.208</i>
	CMEM	NMSE	39.791	97.017	5.023	68.404	13.619
		FB	- 1.941	- 1.875	- 120.235	- 1.908	0.016
		<i>R</i>	<i>- 0.003</i>	<i>0.872</i>	<i>2.086</i>	<i>0.435</i>	<i>0.208</i>

***Errors due to BOOT® software estimations

The *italicized* values are not statistically different from 0 (due to changes in the sign for both lower and upper limits) at 95% CI

EPA Line source of AERMOD model has been used in modeling of different on-road vehicles with varied vehicle volumes and compositions under different meteorological factors and terrain features. Furthermore, additional modeling study will be required to incorporate the effects of complex terrain features of Muscat on the pollutants concentration levels.

Conclusions

In this study, the concentration levels of CO and NO_x were predicted across six different major roads with various traffic vehicle categories and volumes in Muscat using US EPA Line source tool of AERMOD dispersion modeling system. Two different emission factor models (COPERT IV and CMEM) were established based on fleet composition, weight emission standards, vehicle specifications, abatement technologies, fuel types, temperature conditions, and driving behaviors. Studies have proved that the near-road TRAP estimations were attributed to street level environment and specific conditions including low winds, LDV vehicles only, and limited receptors

only. Hence, the field monitoring campaign of CO and NO_x along the roads under normal traffic, road, and meteorological conditions were conducted to help in the validation of the modeled results. The results proved that the predicted and the measured CO and NO_x were within the acceptable limit set by US EPA. However, certain locations were found to have exceeded the standard, especially from high NO_x levels. Also, the overall performance of the predicted concentrations with the measured data was moderate, except some locations that showed significant over/under prediction as well as the poor performance with the measured values. Taking into consideration the overall primary model performance measures, the study found COPERT emission factors showing moderate prediction compared to the CMEM; this may be due to the limited local (arid) vehicle second-by-second velocity and acceleration rate input data of the CMEM model. However, the bootstrap 95% CI estimates over all the performance measures (NMSE, FB, and R) of between model (COPERT–CMEM) comparison for both CO and NO_x were statistically significant from 0 across all the model locations. For the individual model comparison, bootstrap 95% CI estimates over NMSE and FB were the most dominant statistical measures that were

Table 13 Intra-model (between models) comparison using bootstrap CI estimates over NMSE, FB, and R for CO and NOx

Locations	Models	Measures	Lower limits	Upper limits	Student's <i>t</i> test	Mean	SD
Student's <i>t</i> test at 95% CI for CO							
ALK	COPERT-CMEM	NMSE	1.577	7.706	3.141	4.641	1.478
		FB	-2.208	-2.032	-49.889	-2.12	0.042
		R	0.000	0.000	0.171	0.000	0.000
AMT	COPERT-CMEM	NMSE	-841.922	-419.542	-6.179	-630.732	102.074
		FB	-2.573	-1.945	-14.893	-2.259	0.152
		R	0.000	0.000	-0.884	0.000	0.000
ASB	COPERT-CMEM	NMSE	-52.696	-29.45	-7.311	-41.073	5.618
		FB	-1.65	-1.19	-12.76	-1.42	0.111
		R	0.000	0.000	0.447	0.000	0.000
MRA	COPERT-CMEM	NMSE	0.372	3.637	2.54	2.004	0.789
		FB	-1.52	-1.429	-67.145	-1.475	0.022
		R	0.000	0.000	-0.213	0.000	0.000
RWI	COPERT-CMEM	NMSE	5.848	14.375	4.907	10.112	2.061
		FB	-0.638	-0.406	-9.321	-0.522	0.056
		R	0.000	0.000	-0.229	0.000	0.000
RSL	COPERT-CMEM	NMSE	8.998	37.243	3.44	23.121	6.722
		FB	-1.477	-0.87	-8.113	-1.174	0.145
		R	0.000	0.000	-0.799	0.000	0.000
Student's <i>t</i> test at 95% CI for NOx							
ALK	COPERT-CMEM	NMSE	273.585	542.662	6.291	408.123	64.869
		FB	-0.66	-0.385	-7.865	-0.523	0.066
		R	0.000	0.000	-0.234	0.000	0.000
AMT	COPERT-CMEM	NMSE	251.217	743.201	4.182	497.209	118.894
		FB	-3.874	-3.758	-136.146	-3.816	0.028
		R	0.000	0.000	-0.513	0.000	0.000
ASB	COPERT-CMEM	NMSE	149.507	294.692	6.33	222.099	35.086
		FB	-2.657	-2.088	-17.238	-2.373	0.138
		R	0.000	0.000	0.127	0.000	0.000
MRA	COPERT-CMEM	NMSE	2921.552	6149.136	5.815	4535.344	35.613
		FB	-0.362	-0.186	-6.476	-0.274	0.042
		R	0.000	0.000	-0.211	0.000	0.000
RWI	COPERT-CMEM	NMSE	1297.453	2616.223	6.14	1956.838	47.051
		FB	-0.011	-0.005	-5.432	-0.008	0.002
		R	0.000	0.000	-0.619	0.000	0.000
RSL	COPERT-CMEM	NMSE	901.076	2143.705	5.148	1522.391	99.779
		FB	-0.12	-0.056	-5.843	-0.088	0.015
		R	0.000	0.000	0.391	0.000	0.000

significantly different from 0 for both models. The contribution of the complex and varied geographical landscape features in Muscat on traffic emission levels was not considered under this study, except road geometry (road length and width), as the model could not account for the effect of complex and hilly terrain features. The major limitation of the model validation was due to the lack of reliable background CO and NOx data in addition to the emissions from other roads which were not a part of the study.

This is the most and the only comprehensive study conducted in Muscat urban and industrial areas, which was supported by the Omani government. As a result of this study, the government aimed to map air pollution hot spots and set up a permanent network of air pollution monitoring stations around the city. The reported results, which are supported by high-quality dataset, would be an essential infrastructure for emission forecasting, which provides a basis for future urban and city-scale air pollution studies and it can be expanded into

future health and epidemiologic impact assessments. In the case of arid environments in developing countries, the methodology followed in this study can be utilized in other countries with similar environmental climate, such as developing countries in the Middle East; Belize and El Salvador in Central America; Peru (Southern America); and Arizona, Texas, and Oklahoma in the USA (Checkley et al. 2000; Heusinger and Sailor 2019; Song et al. 2017). This study would contribute to enriching the existing body knowledge and in future studies to filling this particular gap in knowledge. Future traffic modeling study may have the high potential of improving the prediction of traffic emissions for accurate exposure assessment in residential areas in Muscat and Oman at large. Finally, a dynamic model evaluation approach involving detailed meteorological information should be considered for future study.

Funding information The authors received the support provided by the Ministry of Environment and Climatic Affairs (MECA), Oman, under the Grant No. CR/DVC/CESAR/16/05.

Compliance with ethical standards

Conflict of interest The authors declare that they have no conflict of interest.

References

- Abdul-Wahab SA, Fadlallah SO (2014) A study of the effects of vehicle emissions on the atmosphere of Sultan Qaboos University in Oman. *Atmos Environ* 98:158–167
- Abou-Senna H, Radwan E, Westerlund K, Cooper CD (2013) Using a traffic simulation model (VISSIM) with an emissions model (MOVES) to predict emissions from vehicles on a limited-access highway. *J Air Waste Manage Assoc* 63:819–831
- Agudelo-Castaneda DM, Calesso Teixeira E, Norte Pereira F (2014) Time-series analysis of surface ozone and nitrogen oxides concentrations in an urban area at Brazil. *Atmos Pollut Res* 5:411–420
- Amoatey P, Sulaiman H (2017) Options for greenhouse gas mitigation strategies for road transportation in Oman. *Am J Clim Chang* 06: 217–229
- Amoatey P, Omidvarborna H, Affum HA, Baawain M (2018a) Performance of AERMOD and CALPUFF models on SO₂ and NO₂ emissions for future health risk assessment in Tema Metropolis. *Hum Ecol Risk Assess* 25:772–786
- Amoatey P, Sulaiman H, Kwarteng A, Al-Reasi HA (2018b) Above-ground carbon dynamics in different arid urban green spaces. *Environ Earth Sci* 77(12):1–10
- Amoatey P, Omidvarborna H, Baawain MS, Al-Mamun A (2019) Emissions and exposure assessments of SO_x, NO_x, PM_{10/2.5} and trace metals from oil industries: a review study (2000–2018). *Process Saf Environ* 123:215–228
- Baawain MS, Al-Serhi AS (2014) Systematic approach for the prediction of ground-level air pollution (around an industrial port) using an artificial neural network. *Aerosol Air Qual Res* 14:124–134
- Bodisco TA, Rahman SMA, Hossain FM, Brown RJ (2019) On-road NO_x emissions of a modern commercial light-duty diesel vehicle using a blend of tyre oil and diesel. *Energy Rep* 5:349–356
- Borrego C, Amorim JH, Tchepel O, Dias D, Rafael S, Sá E, Pimentel C, Fontes T, Fernandes P, Pereira SR, Bandeira JM, Coelho MC (2016) Urban scale air quality modelling using detailed traffic emissions estimates. *Atmos Environ* 131:341–351
- Bowatte G, Lodge CJ, Knibbs LD, Erbas B, Perret JL, Jalaludin B, Morgan GG, Bui DS, Giles GG, Hamilton GS, Wood-Baker R, Thomas P, Thompson BR, Matheson MC, Abramson MJ, Walters EH, Dharmage SC (2018) Traffic related air pollution and development and persistence of asthma and low lung function. *Environ Int* 113:170–176
- Breeze (2019) Meteorological analysis. Breeze AERMOD. <https://www.breeze-software.com/data/meteorological-analysis/>, Accessed 6/5/2019
- Cai H, Xie S (2011) Traffic-related air pollution modeling during the 2008 Beijing Olympic Games: the effects of an odd-even day traffic restriction scheme. *Sci Total Environ* 409:1935–1948
- Cai Y, Hodgson S, Blangiardo M, Gulliver J, Morley D, Fecht D, Vienneau D, de Hoogh K, Key T, Hveem K, Elliott P, Hansell AL (2018) Road traffic noise, air pollution and incident cardiovascular disease: a joint analysis of the HUNT, EPIC-Oxford and UK Biobank cohorts. *Environ Int* 114:191–201
- Chang JC, Hanna SR (2004) Air quality model performance evaluation. *Meteorol Atmos Phys* 87:167–196
- Charabi Y, Abdul-Wahab S, Al-Rawas G, Al-Wardy M, Fadlallah S (2018) Investigating the impact of monsoon season on the dispersion of pollutants emitted from vehicles: a case study of Salalah City, Sultanate of Oman. *Transport Res D - TR E* 59:108–120
- Checkley W, Epstein LD, Gilman RH, Figueroa D, Cama RI, Patz JA, Black RE (2000) Effects of El Niño and ambient temperature on hospital admissions for diarrhoeal diseases in Peruvian children. *Lancet* 355:442–450
- Directorate General of Meteorology (2019) Current local weather. Directorate General of Meteorology. <http://www.met.gov.om/opencms/export/sites/default/dgman/en/home/index.html>. Accessed 4/5/2019 2019
- Gokhale S, Pandian S (2007) A semi-empirical box modeling approach for predicting the carbon monoxide concentrations at an urban traffic intersection. *Atmos Environ* 41:7940–7950
- Halonen JI, Blangiardo M, Toledano MB, Fecht D, Gulliver J, Ghosh R, Anderson HR, Beevers SD, Dajnak D, Kelly FJ, Wilkinson P, Tonne C (2016) Is long-term exposure to traffic pollution associated with mortality? A small-area study in London. *Environ Pollut* 208: 25–32
- Heusinger J, Sailor DJ (2019) Heat and cold roses of U.S. cities: a new tool for optimizing urban climate. *Sustain Cities Soc* 51:101777
- Kadiyala A, Kumar A (2012) Guidelines for operational evaluation of air quality models. Lambert Academic Publishing GmbH & Co, Saarbrücken, p 123
- Khreis H, de Hoogh K, Nieuwenhuijsen MJ (2018) Full-chain health impact assessment of traffic-related air pollution and childhood asthma. *Environ Int* 114:365–375
- Ko J, Myung C-L, Park S (2019) Impacts of ambient temperature, DPF regeneration, and traffic congestion on NO_x emissions from a Euro 6-compliant diesel vehicle equipped with an LNT under real-world driving conditions. *Atmos Environ* 200:1–14
- Korfant M, Gogola M (2019) Traffic generation by various types of urban facilities within Slovak Republic. *Transp Res Proc* 40:310–316
- Kumar A, Bellam NK, Sud A (2012) Performance of an industrial source complex model: predicting long-term concentrations in an urban area. *Environ Prog* 18:93–100
- Kwarteng AY, Dorvlo AS, Vijaya Kumar GT (2009) Analysis of a 27-year rainfall data (1977–2003) in the Sultanate of Oman. *Int J Climatol* 29:605–617
- Liang D et al (2018) Errors associated with the use of roadside monitoring in the estimation of acute traffic pollutant-related health effects. *Environ Res* 165:210–219

- Liu H, Rodgers MO, Guensler R (2019) Impact of road grade on vehicle speed-acceleration distribution, emissions and dispersion modeling on freeways. *Transport Res D - TR E* 69:107–122
- López-Pérez E, Hermosilla T, Carot-Sierra J-M, Palau-Salvador G (2019) Spatial determination of traffic CO emissions within street canyons using inverse modelling. *Atmos Pollut Res* 1(0):1140–1147
- Mannucci PM, Franchini M (2017) Health effects of ambient air pollution in developing countries. *Int J Environ Res Public Health* 14:1048
- Milando CW, Batterman SA (2018) Operational evaluation of the RLINE dispersion model for studies of traffic-related air pollutants. *Atmos Environ* 182:213–224
- Mohan M, Bhati S, Sreenivas A, Marrapu P (2011) Performance evaluation of AERMOD and ADMS-urban for total suspended particulate matter concentrations in megacity Delhi. *Aerosol Air Qual Res* 11: 883–894
- Munir S, Habeebullah TM (2018) Vehicular emissions on main roads in Makkah, Saudi Arabia—a dispersion modelling study. *Arab J Geosci* 11:543
- Muscata Municipality (2019) Open data. <https://www.mm.gov.om/Page.aspx?PAID=122#OpenData&MID=128&Slide=True&MoID=72>, Accessed 07/05/2019
- NAEI (2019) Emission factors for transport National Atmospheric Emission Inventory <http://naei.beis.gov.uk/data/ef-transport>. 08/05/2019
- National Centre for Statistics and Information (2018) Statistical yearbook 2018: issue 46. National Centre for Statistics and Information (NC SI). <https://www.ncsi.gov.om/Elibrary/Pages/LibraryContentDetails.aspx?ItemID=GxJuqSZUD0v4K7T%2FPJp13A%3D%3D>. Accessed 02/05/2019
- Omidvarboma H, Baawain M, Al-Mamun A (2018) Ambient air quality and exposure assessment study of the Gulf Cooperation Council countries: a critical review. *Sci Total Environ* 636:437–448
- Pedersen M, Olsen SF, Halldorsson TI, Zhang C, Hjortebjerg D, Ketzler M, Grandström C, Sørensen M, Damm P, Langhoff-Roos J, Raaschou-Nielsen O (2017) Gestational diabetes mellitus and exposure to ambient air pollution and road traffic noise: a cohort study. *Environ Int* 108:253–260
- Pelletier G, Rigden M, Kauri LM, Shutt R, Mahmud M, Cakmak S, Kumarathasan P, Thomson EM, Vincent R, Broad G, Liu L, Dales R (2017) Associations between urinary biomarkers of oxidative stress and air pollutants observed in a randomized crossover exposure to steel mill emissions. *Int J Hyg Environ Health* 220:387–394
- Ribeiro AG, Downward GS, Freitas CU, Chiaravalloti Neto F, Cardoso MRA, Latorre MRDO, Hystad P, Vermeulen R, Nardocci AC (2019) Incidence and mortality for respiratory cancer and traffic-related air pollution in Sao Paulo, Brazil. *Environ Res* 170:243–251
- Righi S, Luciali P, Pollini E (2009) Statistical and diagnostic evaluation of the ADMS-Urban model compared with an urban air quality monitoring network. *Atmos Environ* 43:3850–3857
- Rosenlieb EG, McAndrews C, Marshall WE, Troy A (2018) Urban development patterns and exposure to hazardous and protective traffic environments. *J Transp Geogr* 66:125–134
- Song J, Wang Z-H, Myint SW, Wang C (2017) The hysteresis effect on surface-air temperature relationship and its implications to urban planning: an examination in Phoenix, Arizona, USA. *Landscape Urban Plan* 167:198–211
- Triantafyllopoulos G, Dimaratos A, Ntziachristos L, Bernard Y, Dornoff J, Samaras Z (2019) A study on the CO₂ and NO_x emissions performance of Euro 6 diesel vehicles under various chassis dynamometer and on-road conditions including latest regulatory provisions. *Sci Total Environ* 666:337–346
- US EPA (2019) Smog, soot, and other air pollution from transportation. United States Environmental Protection Agency. <https://www.epa.gov/transportation-air-pollution-and-climate-change/smog-soot-and-local-air-pollution>. Accessed May 3 2019
- US EPA (2018a) User's guide for the AERMOD meteorological preprocessor (AERMET). US Environmental Protection Agency. https://www3.epa.gov/ttn/scram/7thconf/aermod/aermet_userguide.pdf. Accessed May 2 2019
- US EPA (2018b) User's guide for the AMS/EPA regulatory model (AERMOD). US Environmental Protection Agency, Washington, D.C
- US EPA (2018c) Primary National Ambient Air Quality Standards (NAAQS) for nitrogen dioxide. US Environmental Protection Agency. <https://www.epa.gov/no2-pollution/primary-national-ambient-air-quality-standards-naaqs-nitrogen-dioxide>. Accessed on 17/04/2020
- Wallace HW, Jobson BT, Erickson MH, McCoskey JK, VanReken TM, Lamb BK, Vaughan JK, Hardy RJ, Cole JL, Strachan SM, Zhang W (2012) Comparison of wintertime CO to NO_x ratios to MOVES and MOBILE6.2 on-road emissions inventories. *Atmos Environ* 63: 289–297
- Weichenthal S, van Rijswijk D, Kulka R, You H, van Ryswyk K, Willey J, Dugandzic R, Sutcliffe R, Moulton J, Baika M, White L, Charland JP, Jessiman B (2015) The impact of a landfill fire on ambient air quality in the north: a case study in Iqaluit, Canada. *Environ Res* 142:46–50
- Wen D, Zhai W, Xiang S, Hu Z, Wei T, Noll KE (2017) Near-roadway monitoring of vehicle emissions as a function of mode of operation for light-duty vehicles. *J Air Waste Manage Assoc* 67:1229–1239
- WHO (2019) Air pollution. World Health Organisation. <https://www.who.int/sustainable-development/transport/health-risks/air-pollution/en/>. Accessed 03/05/2019
- Zhang Y, Ioannou PA (2016) Environmental impact of combined variable speed limit and lane change control: a comparison of MOVES and CMEM model. *IFAC-PapersOnLine* 49:323–328
- Zhang L, Hu X, Qiu R, Lin J (2019) Comparison of real-world emissions of LDGVs of different vehicle emission standards on both mountainous and level roads in China. *Transport Res D - TR E* 69:24–39
- Zhou H, Gao H (2018) The impact of urban morphology on urban transportation mode: a case study of Tokyo. *Case Stud Transp Policy* 8: 197–2015

Publisher's note Springer Nature remains neutral with regard to jurisdictional claims in published maps and institutional affiliations.